

Article

Regularization of the Boundary Equilibrium Bifurcation in Filippov System with Rich Discontinuity Boundaries

Nanbin Cao, Yue Zhang and Xia Liu *

School of Mathematics and Science, Hebei GEO University, Shijiazhuang 050031, China; caonanbin@hgu.edu.cn (N.C.); zy9812232024@163.com (Y.Z.)

* Correspondence: liuxia@hgu.edu.cn

Abstract: This paper studies a particular type of planar Filippov system that consists of two discontinuity boundaries separating the phase plane into three disjoint regions with different dynamics. This type of system has wide applications in various subjects. As an illustration, a plant disease model and an avian-only model are presented, and their bifurcation scenarios are investigated. By means of the regularization approach, the blowing up method, and the singular perturbation theory, we provide a different way to analyze the dynamics of this type of Filippov system. In particular, the boundary equilibrium bifurcations of such systems are studied. As a consequence, the nonsmooth fold bifurcation becomes a saddle-node bifurcation, while the persistence bifurcation disappears after regularization.

Keywords: Filippov system; boundary equilibrium bifurcation; regularization; blow up; singular perturbation theory

MSC: 34A36; 34C23; 34D15; 37N25



Citation: Cao, N.; Zhang, Y.; Liu, X. Regularization of the Boundary Equilibrium Bifurcation in Filippov System with Rich Discontinuity Boundaries. *Axioms* **2024**, *13*, 186. <https://doi.org/10.3390/axioms13030186>

Academic Editor: Chris Goodrich

Received: 15 February 2024

Revised: 10 March 2024

Accepted: 11 March 2024

Published: 12 March 2024



Copyright: © 2024 by the authors. Licensee MDPI, Basel, Switzerland. This article is an open access article distributed under the terms and conditions of the Creative Commons Attribution (CC BY) license (<https://creativecommons.org/licenses/by/4.0/>).

1. Introduction

The Filippov system has been widely applied in many subjects, such as biology, electrical engineering, automatic control, and so on [1–6]. A Filippov system is a discontinuous dynamical system composed of two or more smooth vector fields that are separated by discontinuity boundaries [1,7]. In particular, the Filippov system consisting of one discontinuity boundary that separates the phase plane into two regions has been widely studied; see, for instance, [5,7–10]. There are also some analyses of the Filippov system with two discontinuity boundaries separating \mathbb{R}^2 into four regions; see [11–14]. Recently, some work on a Filippov system with two discontinuity boundaries separating \mathbb{R}^2 into three regions attracted our attention [15,16].

The case with three regions has fruitful applications in the real world. For example, such a Filippov plant disease model can help us understand disease transmission dynamics and provide economic and environmentally acceptable control strategies [15]. An avian-only model that incorporates culling off the infected and susceptible birds can also be described by a Filippov system with two discontinuity boundaries separating \mathbb{R}^2 into three regions [16].

The inspiration for this work is the work by Chen [15] and Yang [16], where the stability of different types of equilibria of such a Filippov system is studied. However, the bifurcation analysis of such systems is rare, particularly the boundary equilibrium bifurcation. In fact, boundary equilibrium bifurcations of Filippov systems have received more and more attention in the past decades [2,16–20]. In this work, we investigate the boundary equilibrium bifurcations of Filippov systems with two discontinuity boundaries. Instead of the classical Filippov convention, we choose the regularization method to study the dynamics of such systems, which enables us to build up a relationship between discontinuity-induced bifurcations and smooth bifurcations. The analysis of the present

work shows that the equilibrium bifurcation either becomes a saddle-node bifurcation or disappears after regularization.

There are different ways to regularize a Filippov system [21–27]. In this work, we chose the method introduced by Sotomayor and Teixeira [27]. This method has already been applied to the case where the discontinuity boundary divides \mathbb{R}^2 into two regions [28–36] and into four regions [11,14,37]. However, according to the authors’ knowledge, they have not been applied to the case with three regions, which have more applications in reality.

In the process of regularization, the singular perturbation theory and blowing up technique play an important role. As we see in Section 3, the regularized system R_Z can be reduced to a singular perturbation problem after a scaling transformation. The regularized system is characterized by two time scales, slow time t and fast time τ , which are related by $\tau = t/\varepsilon$. The slow-time system defines a reduced system for $\varepsilon = 0$ [28]. The dynamics of the singular perturbation problem are obtained by combining the two distinguished limits at $\varepsilon = 0$: the slow-time dynamics and the fast-time dynamics.

The structure of this paper is organized as follows: The next section is an overview of the Filippov system with rich discontinuity boundaries, different types of equilibria, the regularization method, and the geometric singular perturbation theory. Additionally, the definition of persistence bifurcation and nonsmooth fold bifurcation are given. In Section 3, we present the main results of this work. The bifurcation analysis of a Filippov plant disease model and its corresponding regularization are investigated in Section 3.1. The bifurcations and phase portraits of a Filippov avian-only model and its corresponding regularization are presented in Section 3.2. In Section 4, we summarize the main results of this paper and point out the future direction.

2. Preliminaries

The definition of a Filippov system that has rich boundaries, different types of equilibria, the regularization method, and two kinds of boundary equilibrium bifurcations is introduced in this section.

2.1. Definition of a Filippov System with Rich Boundaries

The planar Filippov system with one discontinuity boundary that separates \mathbb{R}^2 into two regions has been widely studied in much of the literature; see its definition, for instance, in [3,5,38,39]. In this paper, we study the planar Filippov system with two discontinuity boundaries that separates \mathbb{R}^2 into three regions, that is,

$$Z(X) = \begin{cases} F_1(X), & \text{if } X \in G_1, \\ F_2(X), & \text{if } X \in G_2, \\ F_3(X), & \text{if } X \in G_3, \end{cases} \tag{1}$$

where $X = (x, y) \in \mathbb{R}^2$. The vector fields F_1, F_2, F_3 are given by $F_1 = (f_1, g_1), F_2 = (f_2, g_2), F_3 = (f_3, g_3)$. The discontinuity set Σ is composed of two parts:

$$\Sigma_1 = \{X \in \mathbb{R}^2 : H_1(X) = 0\}, \quad \Sigma_2 = \{X \in \mathbb{R}^2 : H_2(X) = 0, H_1(X) \geq 0\},$$

where H_1, H_2 are smooth scalar functions. For instance, here, we consider $H_1(X) = y - y_0, H_2(X) = x - x_0$. The intersection of the discontinuity boundaries Σ_1 and Σ_2 is the point (x_0, y_0) . The boundaries separate \mathbb{R}^2 into three regions, G_1, G_2 , and G_3 , defined as

$$\begin{aligned} G_1 &= \{X \in \mathbb{R}^2 : H_1(X) < 0\} = \{X \in \mathbb{R}^2 : y < y_0\}, \\ G_2 &= \{X \in \mathbb{R}^2 : H_1(X) > 0, H_2(X) < 0\} = \{X \in \mathbb{R}^2 : y > y_0, x < x_0\}, \\ G_3 &= \{X \in \mathbb{R}^2 : H_1(X) > 0, H_2(X) > 0\} = \{X \in \mathbb{R}^2 : y > y_0, x > x_0\}. \end{aligned}$$

For convenience, we use the following notations in the subsequent discussion:

$$\begin{aligned} \Sigma_{+,y_0} &= \{(x, y_0) | x > x_0\}, & \Sigma_{-,y_0} &= \{(x, y_0) | x < x_0\}, \\ \Sigma_{x_0,+} &= \{(x_0, y) | y > y_0\}, & \Sigma_{x_0,y_0} &= \{(x_0, y_0)\}. \end{aligned}$$

Notice that $\Sigma_1 = \Sigma_{+,y_0} \cup \Sigma_{-,y_0} \cup \Sigma_{x_0,y_0}$ and $\Sigma_2 = \Sigma_{x_0,+} \cup \Sigma_{x_0,y_0}$. The distribution of \mathbb{R}^2 by the discontinuity boundaries is presented in Figure 1.

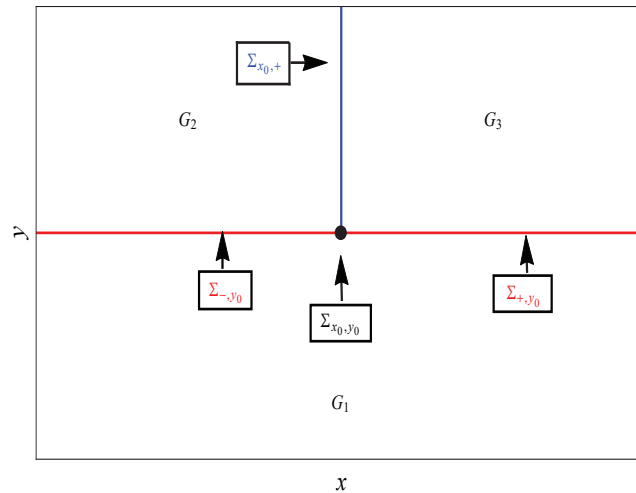


Figure 1. The discontinuity set separates \mathbb{R}^2 into three regions G_1, G_2, G_3 .

With the above notations, $Z(X)$ can be rewritten as the general Filippov system $Z(X) = (Z_1(X), Z_2(X), Z_3(X))$, where

$$Z_1(X) = \begin{cases} F_1(X), & \text{if } X \in G_1, \\ F_3(X), & \text{if } X \in G_3, \end{cases}$$

with the discontinuity boundary Σ_{+,y_0} ,

$$Z_2(X) = \begin{cases} F_1(X), & \text{if } X \in G_1, \\ F_2(X), & \text{if } X \in G_2, \end{cases}$$

with the discontinuity boundary Σ_{-,y_0} , and

$$Z_3(X) = \begin{cases} F_2(X), & \text{if } X \in G_2, \\ F_3(X), & \text{if } X \in G_3, \end{cases}$$

with the discontinuity boundary $\Sigma_{x_0,+}$. The dynamics of Z in G_1, G_2 , and G_3 are defined by the flows of F_1, F_2 , and F_3 , respectively. The dynamics of the discontinuity boundaries are defined in the usual way. Here, we take the subsystem Z_3 as an example to define its dynamics when $X \in \Sigma_{x_0,+}$. Following [1], the boundary $\Sigma_{x_0,+}$ is divided into the following:

- The sliding region: $\Sigma_{x_0,+}^s = \{X \in \Sigma_{x_0,+} : (H_2F_2(X)) \cdot (H_2F_3(X)) \leq 0\}$,
- The crossing region: $\Sigma_{x_0,+}^c = \{X \in \Sigma_{x_0,+} : (H_2F_2(X)) \cdot (H_2F_3(X)) > 0\}$,

where $H_2F_i = \left(\frac{\partial H_2}{\partial x}, \frac{\partial H_2}{\partial y} \right) \cdot (f_i, g_i), i = 2, 3$.

On the sliding region $\Sigma_{x_0,+}^s$, the sliding vector field F_{23} is defined by the Filippov's convex method [7] as

$$F_{23} = (1 - \lambda_{23})F_2 + \lambda_{23}F_3, \tag{2}$$

where

$$\lambda_{23}(X) = \frac{H_2 F_2(X)}{H_2(F_2 - F_3)(X)}, \quad 0 \leq \lambda_{23} \leq 1.$$

In a similar way, the sliding vector fields F_{12} and F_{13} are defined as

$$F_{12} = (1 - \lambda_{12})F_1 + \lambda_{12}F_2 \quad \text{with} \quad \lambda_{12}(X) = \frac{H_1 F_1(X)}{H_1(F_1 - F_2)(X)},$$

$$F_{13} = (1 - \lambda_{13})F_1 + \lambda_{13}F_3 \quad \text{with} \quad \lambda_{13}(X) = \frac{H_1 F_1(X)}{H_1(F_1 - F_3)(X)}.$$

2.2. Definition of Equilibria

This part distinguishes different types of equilibria in the Filippov system (1).

Definition 1 (Admissible equilibrium). *A point $X \in G = G_1 \cup G_2 \cup G_3$ is an admissible equilibrium of (1) if*

$$F_i(X) = 0, \quad X \in G_i,$$

where $i = 1, 2, 3$.

Definition 2 (Pseudo-equilibrium). *A point \tilde{X} is a pseudoequilibrium of (1) if it is an equilibrium of the sliding vector fields F_{12}, F_{13} , or F_{23} , i.e.,*

$$F_{12}(\tilde{X}) = 0, \quad \tilde{X} \in \Sigma_{-,y_0}^s,$$

or

$$F_{13}(\tilde{X}) = 0, \quad \tilde{X} \in \Sigma_{+,y_0}^s,$$

or

$$F_{23}(\tilde{X}) = 0, \quad \tilde{X} \in \Sigma_{x_0,+}^s.$$

Here, $\Sigma_{-,y_0}^s, \Sigma_{+,y_0}^s$ denote the sliding region on the boundary $\Sigma_{-,y_0}, \Sigma_{+,y_0}$, respectively.

Definition 3 (Boundary equilibrium). *A point \hat{X} is termed as a boundary equilibrium of (1) on Σ_{-,y_0} if*

$$\begin{aligned} &F_1(\hat{X}) = 0 \quad \text{and} \quad H_1(\hat{X}) = 0, \\ \text{or} \quad &F_2(\hat{X}) = 0 \quad \text{and} \quad H_1(\hat{X}) = 0; \end{aligned}$$

a boundary equilibrium on Σ_{+,y_0} if

$$\begin{aligned} &F_1(\hat{X}) = 0 \quad \text{and} \quad H_1(\hat{X}) = 0, \\ \text{or} \quad &F_3(\hat{X}) = 0 \quad \text{and} \quad H_1(\hat{X}) = 0; \end{aligned}$$

a boundary equilibrium on $\Sigma_{x_0,+}$ if

$$\begin{aligned} &F_2(\hat{X}) = 0 \quad \text{and} \quad H_2(\hat{X}) = 0, \\ \text{or} \quad &F_3(\hat{X}) = 0 \quad \text{and} \quad H_2(\hat{X}) = 0. \end{aligned}$$

2.3. Description of the Regularization Method

The regularization method provides a different way to study the dynamics of Filippov systems. The regularization of a Filippov system is a smooth approximation of the Filippov system that removes the discontinuities. Therefore, the regularization makes it possible to construct a relationship between the Filippov systems and smooth systems.

In this section, we briefly review the regularization method proposed in [27]. It should be noticed that for system (1), the discontinuity boundary loses smoothness at the

intersection point (x_0, y_0) . It needs additional blow-up before applying the regularization method, which is shown more detail in Section 3.

Definition 4. A C^∞ function $\varphi : \mathbb{R} \rightarrow \mathbb{R}$ is a transition function if $\varphi(x) = -1$ for $x \leq -1$, $\varphi(x) = 1$ for $x \geq 1$ and $\varphi'(x) > 0$ if $x \in (-1, 1)$.

Given a Filippov system

$$Z(X) = \begin{cases} F(X), & \text{if } H(X) < 0, \\ G(X), & \text{if } H(X) > 0, \end{cases} \tag{3}$$

where $H(X)$ is a smooth scalar function, and the discontinuity boundary is $\Sigma = \{X \in \mathbb{R}^2 : H(X) = 0\}$, the regularization of (3) is a 1-parameter family given by

$$R_Z(X) = \left(\frac{1}{2} + \frac{\varphi_\varepsilon(H(X))}{2}\right)G(X) + \left(\frac{1}{2} - \frac{\varphi_\varepsilon(H(X))}{2}\right)F(X), \tag{4}$$

with $\varphi_\varepsilon(x) = \varphi\left(\frac{x}{\varepsilon}\right)$ for $\varepsilon > 0$.

2.4. Geometric Singular Perturbation Theory

Geometric singular perturbation theory (GSPT) is an important tool in the field of continuous dynamical systems. A singular perturbation problem in \mathbb{R}^2 is a differential system which can be written as

$$x' = dx/d\tau = f(x, y, \varepsilon), \quad y' = dy/d\tau = \varepsilon g(x, y, \varepsilon), \tag{5}$$

or equivalently, after the time rescaling $t = \varepsilon\tau$,

$$\varepsilon \dot{x} = dx/dt = f(x, y, \varepsilon), \quad \dot{y} = dy/dt = g(x, y, \varepsilon), \tag{6}$$

where $(x, y) \in \mathbb{R}^2$, f, g are smooth functions. Here, system (5) is called the fast system. System (6) is called the slow system. Observe that for $\varepsilon > 0$, the phase portraits of the fast and the slow systems coincide. When $\varepsilon = 0$, the set

$$\mathcal{M} = \{(x, y) : f(x, y, 0) = 0\} \tag{7}$$

consists of all the equilibria of the fast system. We call \mathcal{M} the slow manifold of the singular perturbation problem. A point $p \in \mathcal{M}$ is said to be normally hyperbolic if $\left.\frac{\partial f}{\partial x}\right|_p \neq 0$.

Notice that when $\varepsilon = 0$, the slow system defines a dynamical system on \mathcal{M} , called the reduced problem:

$$f(x, y, 0) = 0, \quad \dot{y} = g(x, y, 0). \tag{8}$$

Combining results on the dynamics of these two limiting problems, one obtains information on the dynamics for small values of ε ; more details are provided in [28].

2.5. Description of the Boundary Equilibrium Bifurcations

The two types of boundary equilibrium bifurcations discussed in this work are given here. More details about these bifurcations can be found in [1,20,40].

- *Boundary Equilibrium Bifurcations:*

1. *Persistence:*

A branch of admissible equilibria firstly turns into a boundary equilibrium, and then a branch of pseudoequilibria as the parameter varies;

2. *Nonsmooth fold bifurcation:*

A branch of admissible equilibria collides with a pseudoequilibrium, then becomes a boundary point, and then both disappear as the parameter varies.

3. Main Results and Examples

Since system (1) is composed of several parts of boundaries, that is, $\Sigma = \Sigma_{+,y_0} \cup \Sigma_{-,y_0} \cup \Sigma_{x_0,+} \cup \Sigma_{x_0,y_0}$, we have to apply the regularization method to each part separately. Notice that the boundaries lose smoothness at Σ_{x_0,y_0} , or the point (x_0, y_0) , so this point needs additional consideration, which is explained by specific examples in the next section. Here, we only present the formula for regularizing system (1) at the boundaries Σ_{+,y_0} , Σ_{-,y_0} , and $\Sigma_{x_0,+}$.

Recall that system (1) can be written as $Z(X) = (Z_1(X), Z_2(X), Z_3(X))$ with the boundaries Σ_{+,y_0} , Σ_{-,y_0} , $\Sigma_{x_0,+}$. Next, we apply the regularization method in [27] to the subsystems $Z_1(X)$, $Z_2(X)$, and $Z_3(X)$.

1. For the subsystem Z_1 with the boundary $y = y_0, x > x_0$, its regularization is given by

$$R_{Z_1} = \left[\frac{1}{2} + \frac{1}{2} \varphi \left(\frac{y - y_0}{\varepsilon} \right) \right] F_3(x, y) + \left[\frac{1}{2} - \frac{1}{2} \varphi \left(\frac{y - y_0}{\varepsilon} \right) \right] F_1(x, y). \tag{9}$$

2. For Z_2 with the boundary $y = y_0, x < x_0$, its regularization is

$$R_{Z_2} = \left[\frac{1}{2} + \frac{1}{2} \varphi \left(\frac{y - y_0}{\varepsilon} \right) \right] F_2(x, y) + \left[\frac{1}{2} - \frac{1}{2} \varphi \left(\frac{y - y_0}{\varepsilon} \right) \right] F_1(x, y). \tag{10}$$

3. For Z_3 with the boundary $x = x_0, y > y_0$, its regularization is

$$R_{Z_3} = \left[\frac{1}{2} + \frac{1}{2} \varphi \left(\frac{x - x_0}{\varepsilon} \right) \right] F_3(x, y) + \left[\frac{1}{2} - \frac{1}{2} \varphi \left(\frac{x - x_0}{\varepsilon} \right) \right] F_2(x, y). \tag{11}$$

For the subsystem R_{Z_1} , assuming $u = (y - y_0)/\varepsilon$, system (9) can be written as a singular perturbation problem

$$\frac{d}{dt} \begin{pmatrix} x \\ \varepsilon u \end{pmatrix} = \begin{pmatrix} \frac{1}{2}(f_1(x, y) + f_3(x, y)) + \frac{\varphi(u)}{2}(f_3(x, y) - f_1(x, y)) \\ \frac{1}{2}(g_1(x, y) + g_3(x, y)) + \frac{\varphi(u)}{2}(g_3(x, y) - g_1(x, y)) \end{pmatrix}. \tag{12}$$

By rescaling time by $\tau = t/\varepsilon$, system (12) becomes

$$\frac{d}{d\tau} \begin{pmatrix} x \\ u \end{pmatrix} = \begin{pmatrix} \varepsilon \left[\frac{1}{2}(f_1(x, y) + f_3(x, y)) + \frac{\varphi(u)}{2}(f_3(x, y) - f_1(x, y)) \right] \\ \frac{1}{2}(g_1(x, y) + g_3(x, y)) + \frac{\varphi(u)}{2}(g_3(x, y) - g_1(x, y)) \end{pmatrix}. \tag{13}$$

The slow manifold \mathcal{M}_1 is given by

$$\mathcal{M}_1 = \left\{ (u, y) : \frac{1}{2}(g_1(x, y) + g_3(x, y)) + \frac{\varphi(u)}{2}(g_3(x, y) - g_1(x, y)) = 0 \right\}.$$

Then, the slow system (12) defines a dynamical system on \mathcal{M}_1

$$\begin{pmatrix} dx/dt \\ 0 \end{pmatrix} = \begin{pmatrix} \frac{1}{2}(f_1(x, y) + f_3(x, y)) + \frac{\varphi(u)}{2}(f_3(x, y) - f_1(x, y)) \\ \frac{1}{2}(g_1(x, y) + g_3(x, y)) + \frac{\varphi(u)}{2}(g_3(x, y) - g_1(x, y)) \end{pmatrix}.$$

In a similar way, we derive the slow manifold \mathcal{M}_2 for system R_{Z_2}

$$\mathcal{M}_2 = \left\{ (u, y) : \frac{1}{2}(g_1(x, y) + g_2(x, y)) + \frac{\varphi(u)}{2}(g_2(x, y) - g_1(x, y)) = 0 \right\},$$

and the reduced problem

$$\begin{pmatrix} dx/dt \\ 0 \end{pmatrix} = \begin{pmatrix} \frac{1}{2}(f_1(x, y) + f_2(x, y)) + \frac{\varphi(u)}{2}(f_2(x, y) - f_1(x, y)) \\ \frac{1}{2}(g_1(x, y) + g_2(x, y)) + \frac{\varphi(u)}{2}(g_2(x, y) - g_1(x, y)) \end{pmatrix}.$$

For system (11), suppose $v = (x - x_0)/\epsilon$, then it becomes

$$\frac{d}{dt} \begin{pmatrix} \epsilon v \\ y \end{pmatrix} = \begin{pmatrix} \frac{1}{2}(f_2(x, y) + f_3(x, y)) + \frac{\varphi(v)}{2}(f_3(x, y) - f_2(x, y)) \\ \frac{1}{2}(g_2(x, y) + g_3(x, y)) + \frac{\varphi(v)}{2}(g_3(x, y) - g_2(x, y)) \end{pmatrix}. \tag{14}$$

Rescaling time by $\tau = t/\epsilon$, system (14) becomes

$$\frac{d}{d\tau} \begin{pmatrix} v \\ y \end{pmatrix} = \begin{pmatrix} \frac{1}{2}(f_2(x, y) + f_3(x, y)) + \frac{\varphi(v)}{2}(f_3(x, y) - f_2(x, y)) \\ \epsilon \left[\frac{1}{2}(g_2(x, y) + g_3(x, y)) + \frac{\varphi(v)}{2}(g_3(x, y) - g_2(x, y)) \right] \end{pmatrix}. \tag{15}$$

The slow manifold \mathcal{M}_3 is given by

$$\mathcal{M}_3 = \left\{ (v, y) : \frac{1}{2}(f_2(x, y) + f_3(x, y)) + \frac{\varphi(v)}{2}(f_3(x, y) - f_2(x, y)) = 0 \right\}.$$

The reduced problem is

$$\begin{pmatrix} 0 \\ dy/dt \end{pmatrix} = \begin{pmatrix} \frac{1}{2}(f_2(x, y) + f_3(x, y)) + \frac{\varphi(v)}{2}(f_3(x, y) - f_2(x, y)) \\ \frac{1}{2}(g_2(x, y) + g_3(x, y)) + \frac{\varphi(v)}{2}(g_3(x, y) - g_2(x, y)) \end{pmatrix}.$$

Comparing the singular perturbation problem with Filippov system (1), we have the following results.

Theorem 1 ([14]). *For the Filippov system $Z_i(X)$ and its regularization $R_{Z_i}(X)$, the trajectories of $R_{Z_i}(X)$ are the solutions of a singular perturbation problem. The sliding region is homeomorphic to the slow manifold, and the sliding vector field F_j is homeomorphic to the reduced problem on \mathcal{M}_i , $i = 1, 2, 3, j = 13, 12, 23$.*

Subsequently, we take two specific examples to illustrate the regularization of the Filippov system with rich discontinuity boundaries.

3.1. The Filippov Plant Disease Model

Plant diseases are currently one of the major threats to crop production and the worldwide economy [41,42]. Many different measures have been implemented to control plant diseases, such as the use of chemicals [43], rogue infected trees [44], and the removal of infected branches [45]. In order to understand the disease transmission dynamics and provide economic and environmentally acceptable control strategies, many mathematical models have been constructed [46]. More recently, a Filippov plant disease model that incorporates cutting off infected branches and replanting susceptible trees has been built [15]. The model [15] is constructed based on the following regulations:

1. When $y < y_0$, no control strategy is taken;
2. When $y > y_0, x < x_0$, infected branches are cut off at a rate of $c_1 > 0$, and disease-free trees are replanted at a rate of $d > 0$;
3. When $y > y_0, x > x_0$, infected branches are removed at a rate of $c_2 > 0$,

which can be written as a Filippov system with two boundaries:

$$Z(X) = \begin{cases} F_1(X), & \text{if } X \in G_1, \\ F_2(X), & \text{if } X \in G_2, \\ F_3(X), & \text{if } X \in G_3, \end{cases} \tag{16a}$$

where

$$\begin{aligned} F_1(x, y) &= (ax - \beta xy - \eta x, \beta xy - \delta y), \\ F_2(x, y) &= (ax - \beta xy - \eta x + dx + c_1 y, \beta xy - \delta y - c_1 y), \\ F_3(x, y) &= (ax - \beta xy - \eta x + c_2 y, \beta xy - \delta y - c_2 y), \end{aligned} \tag{16b}$$

and

$$G_1 = \{(x, y) | y < y_0\}, G_2 = \{(x, y) | x < x_0, y > y_0\}, G_3 = \{(x, y) | x > x_0, y > y_0\}. \tag{16c}$$

The discontinuity set Σ consists of two parts:

$$\Sigma_1 = \{X \in \mathbb{R}^2 : y - y_0 = 0\}, \quad \Sigma_2 = \{X \in \mathbb{R}^2 : x - x_0 = 0, y - y_0 \geq 0\}.$$

Here, $x > 0, y > 0$, respectively, represent the number of susceptible and infected trees. a is the planting rate and $a > \eta > 0, \beta > 0$ is the transmission rate. $\eta > 0, \delta > 0$ denote the death rate of the susceptible and infected trees, respectively. $x_0 > 0, y_0 > 0$, respectively, denote the susceptible threshold value and the infected threshold level.

3.1.1. Equilibria and Bifurcation

It is simple to check whether system (16) has two equilibria in region G_i : a saddle equilibrium $E_0(0, 0)$ and an equilibrium $E_i, i = 1, 2, 3$, which can be expressed as

$$\begin{aligned} E_1 &= (x_1, y_1) = \left(\frac{\delta}{\beta}, \frac{a - \eta}{\beta} \right); \\ E_2 &= (x_2, y_2) = \left(\frac{\delta + c_1}{\beta}, \frac{(a - \eta + d)(\delta + c_1)}{\beta \delta} \right); \\ E_3 &= (x_3, y_3) = \left(\frac{\delta + c_2}{\beta}, \frac{(a - \eta)(\delta + c_2)}{\beta \delta} \right). \end{aligned}$$

By straightforward computation, E_1 is a center, while the equilibrium E_i in region G_i is globally asymptotically stable, $i = 2, 3$.

In [15], the authors discuss the stability of all equilibria of 16 different cases based on the values of x_i and $y_i, i = 0, 1, 2, 3$. Instead of the discussion of stability, we focus on the bifurcation analysis in this work. Only the case under the condition

$$\begin{aligned} x_0 < x_1 < x_3 < x_2 \quad \text{with} \quad y_0 < y_1 < y_3 < y_2, \quad \text{or} \quad y_1 < y_0 < y_3 < y_2, \\ \text{or} \quad y_1 < y_3 < y_0 < y_2, \quad \text{or} \quad y_1 < y_3 < y_2 < y_0 \end{aligned} \tag{17}$$

is analyzed; the other cases are similar, so we omit their analysis here. Furthermore, for our analysis, the condition

$$\beta x_0 - c_2 \leq 0, c_1 > c_2, a > \eta \tag{18}$$

is required.

Proposition 1. *A nonsmooth fold bifurcation occurs in system (16) under condition (17). Specifically, the following is performed:*

1. When $x_0 < x_1 < x_3 < x_2$ and $y_1 < y_0 < y_3 < y_2$, system (16) has an asymptotically stable focus, a center equilibrium, and a pseudosaddle;

2. When $x_0 < x_1 < x_3 < x_2$ and $y_0 = y_3$, the center equilibrium is preserved, while the other two points collide and turn into a boundary equilibrium of the vector field F_3 ;
3. When $x_0 < x_1 < x_3 < x_2$ and $y_0 > y_3$, system (16) only has a center equilibrium.

The proof for the existence and stability of each equilibrium is derived from the work in [15]. Then, it is direct to derive the proof of this proposition.

Next, we study the regularization of the plant disease system (16).

3.1.2. Regularization

Definition 5 (Simple discontinuity [11]). *Assuming that there exists a polynomial function T such that $T^{-1}(0) = \Sigma_1 \cup \Sigma_2$, we say that $p \in T^{-1}(0)$ is a simple discontinuity of Z if p is a regular point of T , that is,*

$$\nabla T(p) = \left(\frac{\partial T}{\partial x}(p), \frac{\partial T}{\partial y}(p) \right) \neq (0, 0).$$

According to Definition 5 and taking $T = (x - x_0)(y - y_0)$, the discontinuity set Σ of system (16) can be divided into the simple discontinuity $\Sigma_{+,y_0} \cup \Sigma_{-,y_0} \cup \Sigma_{x_0,+}$ and the nonsimple discontinuity Σ_{x_0,y_0} . The meaning of these notations is referred to Section 2.1. Subsequently, the regularization method [27] is applied separately to each part of the discontinuity set of the Filippov plant disease model (16).

- *Case I.*
For the nonsimple discontinuity Σ_{x_0,y_0} , we first transform it into a simple discontinuity. To this end, we consider the map

$$\phi : S^1 \times \mathbb{R}^+ \rightarrow \mathbb{R}^2, \quad \phi(\theta, r) = (x_0 + r \cos \theta, y_0 + r \sin \theta). \tag{19}$$

Then, the discontinuous vector field induced by ϕ on $S^1 \times \mathbb{R}^+$ has only simple discontinuities, and it is determined by the smooth vector fields \bar{F}_i on $\phi^{-1}(G_i)$, $i = 1, 2, 3$; see Figure 2. More details about the map ϕ are provided in [11,14,47].

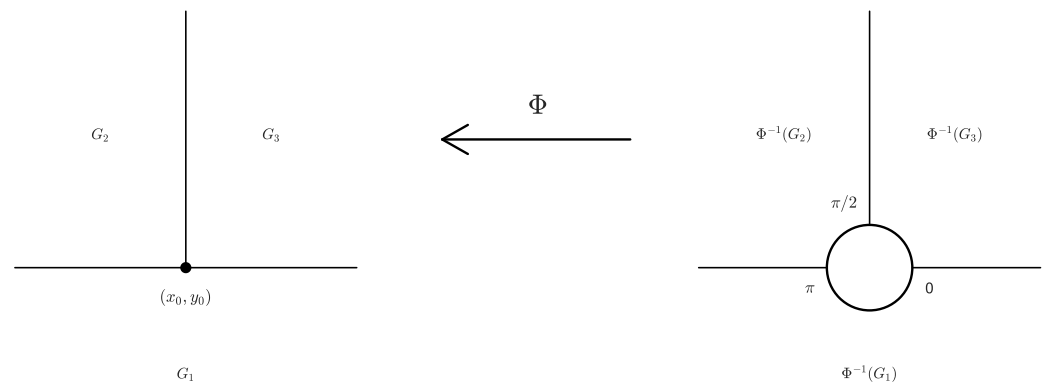


Figure 2. There is a nonsimple discontinuity (x_0, y_0) on the left. There are only simple discontinuities on the right.

The dynamics of the point (x_0, y_0) are given by the map ϕ with $r = 0$. In the new coordinates (r, θ) , it is direct to compute

$$r\dot{\theta} = -f_i \sin \theta + g_i \cos \theta.$$

After performing the time scaling $t = r\tau$, then

$$\theta' = -f_i \sin \theta + g_i \cos \theta,$$

where $F_i = (f_i, g_i), i = 1, 2, 3$. Substituting the specific form of (f_i, g_i) , for $0 < \theta < \pi/2$, $F_3(x, y) = (f_3, g_3) = (ax - \beta xy - \eta x + c_2 y, \beta xy - \delta y - c_2 y)$, the dynamics are given by

$$\theta' = \cos \theta(\beta x_0 y_0 - \delta y_0 - c_2 y_0) - \sin \theta(ax_0 - \beta x_0 y_0 - \eta x_0 + c_2 y_0);$$

for $\pi/2 < \theta < \pi$, $F_2(x, y) = (f_2, g_2) = (ax - \beta xy - \eta x + dx + c_1 y, \beta xy - \delta y - c_1 y)$, the dynamics are

$$\theta' = \cos \theta(\beta x_0 y_0 - \delta y_0 - c_1 y_0) - \sin \theta(ax_0 - \beta x_0 y_0 - \eta x_0 + dx_0 + c_1 y_0);$$

for $\pi < \theta < 2\pi$, $F_1(x, y) = (f_1, g_1) = (ax - \beta xy - \eta x, \beta xy - \delta y)$, the dynamics are

$$\theta' = \cos \theta(\beta x_0 y_0 - \delta y_0) - \sin \theta(ax_0 - \beta x_0 y_0 - \eta x_0).$$

Except for the nonsimple discontinuity Σ_{x_0, y_0} , the regularization method [27] can be applied to the other boundaries directly.

- *Case II.*
For the Filippov system

$$Z_1(x, y) = \begin{cases} F_1(x, y), & (x, y) \in G_1, \\ F_3(x, y), & (x, y) \in G_3, \end{cases}$$

with the boundary $\Sigma_{+, y_0} = \{(x, y_0) | y = y_0, x > x_0\}$. Applying the regularization approach [27], the regularized vector field is

$$R_{Z_1} = \left[\frac{1}{2} + \frac{1}{2} \varphi \left(\frac{y - y_0}{\varepsilon} \right) \right] F_3(x, y) + \left[\frac{1}{2} - \frac{1}{2} \varphi \left(\frac{y - y_0}{\varepsilon} \right) \right] F_1(x, y). \tag{20}$$

That is,

$$\begin{aligned} \dot{x} &= \left[\frac{1}{2} + \frac{1}{2} \varphi \left(\frac{y - y_0}{\varepsilon} \right) \right] (ax - \beta xy - \eta x + c_2 y) + \left[\frac{1}{2} - \frac{1}{2} \varphi \left(\frac{y - y_0}{\varepsilon} \right) \right] (ax - \beta xy) \\ &\quad - \left[\frac{1}{2} - \frac{1}{2} \varphi \left(\frac{y - y_0}{\varepsilon} \right) \right] \eta x \\ &= ax - \beta xy - \eta x + \frac{c_2 y}{2} + \frac{c_2 y}{2} \varphi \left(\frac{y - y_0}{\varepsilon} \right), \\ \dot{y} &= \left[\frac{1}{2} + \frac{1}{2} \varphi \left(\frac{y - y_0}{\varepsilon} \right) \right] (\beta xy - \delta y - c_2 y) + \left[\frac{1}{2} - \frac{1}{2} \varphi \left(\frac{y - y_0}{\varepsilon} \right) \right] (\beta xy - \delta y) \\ &= \beta xy - \delta y - \frac{c_2 y}{2} - \frac{c_2 y}{2} \varphi \left(\frac{y - y_0}{\varepsilon} \right). \end{aligned} \tag{21}$$

System (21) can be transformed into a singular perturbation problem by

$$y = y_0 + \eta \cos \psi, \quad \varepsilon = \eta \sin \psi, \tag{22}$$

where $\eta \geq 0$ and $\psi \in [0, \pi]$, which is

$$\begin{aligned} \eta \dot{\psi} &= -\sin \psi \left[\beta x(y_0 + \eta \cos \psi) - \delta(y_0 + \eta \cos \psi) - \frac{c_2(y_0 + \eta \cos \psi)}{2} \right. \\ &\quad \left. - \frac{c_2(y_0 + \eta \cos \psi)}{2} \varphi(\cot \psi) \right], \\ \dot{x} &= ax - \beta x(y_0 + \eta \cos \psi) - \eta x \\ &\quad + \frac{c_2(y_0 + \eta \cos \psi)}{2} + \frac{c_2(y_0 + \eta \cos \psi)}{2} \varphi(\cot \psi). \end{aligned}$$

Now, $\varepsilon = 0$ is represented by $\eta = 0$. The slow manifold is given by $\mathcal{M}_1 = \left\{ (x, \psi) \in \mathbb{R} \times (0, \pi) : -\sin \psi \left[\beta xy_0 - \delta y_0 - \frac{c_2 y_0}{2} - \frac{\varphi(\cot \psi)}{2} c_2 y_0 \right] = 0 \right\}$, i.e., $\varphi(\cot \psi) = \frac{2\beta xy_0 - 2\delta y_0 - c_2 y_0}{c_2 y_0} = \frac{2\beta x - 2\delta - c_2}{c_2}$. The slow manifold is a curve that connects $(x, \psi) = \left(\frac{\delta + c_2}{\beta}, 0 \right)$ and $(x, \psi) = \left(\frac{\delta}{\beta}, \pi \right)$.

- *Case III.*
For the Filippov system

$$Z_2(x, y) = \begin{cases} F_1(x, y), & (x, y) \in G_1, \\ F_2(x, y), & (x, y) \in G_2, \end{cases}$$

with the boundary $\Sigma_{-,y_0} = \{(x, y_0) | y = y_0, x < x_0\}$, its regularized system is

$$R_{Z_2} = \left[\frac{1}{2} + \frac{1}{2} \varphi \left(\frac{y - y_0}{\varepsilon} \right) \right] F_2(x, y) + \left[\frac{1}{2} - \frac{1}{2} \varphi \left(\frac{y - y_0}{\varepsilon} \right) \right] F_1(x, y), \tag{23}$$

i.e.,

$$\begin{aligned} \dot{x} &= ax - \beta xy - \eta x + \frac{dx + c_1 y}{2} + \frac{dx + c_1 y}{2} \varphi \left(\frac{y - y_0}{\varepsilon} \right), \\ \dot{y} &= \beta xy - \delta y - \frac{c_1 y}{2} - \frac{c_1 y}{2} \varphi \left(\frac{y - y_0}{\varepsilon} \right). \end{aligned} \tag{24}$$

After performing transformation (22), system (24) is transformed into a singular perturbation problem:

$$\begin{aligned} \eta \dot{\psi} &= -\sin \psi \left[\beta x(y_0 + \eta \cos \psi) - \delta(y_0 + \eta \cos \psi) - \frac{c_1(y_0 + \eta \cos \psi)}{2} \right. \\ &\quad \left. - \frac{c_1(y_0 + \eta \cos \psi)}{2} \varphi(\cot \psi) \right], \\ \dot{x} &= ax - \beta x(y_0 + \eta \cos \psi) - \eta x + \frac{dx + c_1(y_0 + \eta \cos \psi)}{2} + \frac{dx}{2} \varphi(\cot \psi) \\ &\quad + \frac{c_1(y_0 + \eta \cos \psi)}{2} \varphi(\cot \psi). \end{aligned}$$

For $\varepsilon = 0$, the slow manifold is given by

$$\mathcal{M}_2 = \left\{ (x, \psi) \in \mathbb{R} \times (0, \pi) : -\sin \psi \left[\beta xy_0 - \delta y_0 - \frac{c_1 y_0}{2} - \frac{c_1 y_0}{2} \varphi(\cot \psi) \right] = 0 \right\},$$

i.e., $\varphi(\cot \psi) = \frac{2\beta x - 2\delta - c_1}{c_1}$. Since our discussion is under the condition $0 < x < x_0$ and $x_0 < x_1 < x_3 < x_2$, it gives $\varphi(\cot \psi) < -1$. Thus, there is no slow manifold.

- *Case IV.*
For the Filippov system

$$Z_3(x, y) = \begin{cases} F_2(x, y), & (x, y) \in G_2, \\ F_3(x, y), & (x, y) \in G_3, \end{cases}$$

with the boundary $\Sigma_{x_0,+} = \{(x_0, y) | x = x_0, y > y_0\}$, the regularized system is

$$R_{Z_3} = \left[\frac{1}{2} + \frac{1}{2} \varphi \left(\frac{x - x_0}{\varepsilon} \right) \right] F_3(x, y) + \left[\frac{1}{2} - \frac{1}{2} \varphi \left(\frac{x - x_0}{\varepsilon} \right) \right] F_2(x, y), \tag{25}$$

i.e.,

$$\begin{aligned} \dot{x} &= ax - \beta xy - \eta x + \frac{dx + c_1y + c_2y}{2} + \frac{c_2y - dx - c_1y}{2} \varphi\left(\frac{x - x_0}{\varepsilon}\right), \\ \dot{y} &= \beta xy - \delta y - \frac{c_1y + c_2y}{2} + \frac{c_1y - c_2y}{2} \varphi\left(\frac{x - x_0}{\varepsilon}\right). \end{aligned} \tag{26}$$

After performing the transformation

$$x = x_0 + \eta \cos \psi, \quad \varepsilon = \eta \sin \psi, \tag{27}$$

where $\eta \geq 0$ and $\psi \in [0, \pi]$, system (26) is changed into a singular perturbation problem

$$\begin{aligned} \eta \dot{\psi} &= -\sin \psi \left[a(x_0 + \eta \cos \psi) - \beta(x_0 + \eta \cos \psi)y - \eta(x_0 + \eta \cos \psi) + \frac{d\eta \cos \psi}{2} \right. \\ &\quad \left. + \frac{c_1y + c_2y + dx_0}{2} + \frac{(c_2y - c_1y - d(x_0 + \eta \cos \psi))}{2} \varphi(\cot \psi) \right], \\ \dot{y} &= \beta(x_0 + \eta \cos \psi)y - \delta y - \frac{c_1y + c_2y}{2} + \frac{c_1y - c_2y}{2} \varphi(\cot \psi). \end{aligned}$$

For $\varepsilon = 0$, the slow manifold is given by

$$\mathcal{M}_3 = \left\{ (\psi, y) \in (0, \pi) \times \mathbb{R} : \right.$$

$$\left. -\sin \psi \left[ax_0 - \beta x_0 y - \eta x_0 + \frac{dx_0}{2} + \frac{c_1y + c_2y}{2} + \frac{c_2y - dx_0 - c_1y}{2} \varphi(\cot \psi) \right] = 0 \right\},$$

i.e., $\varphi(\cot \psi) = \frac{2ax_0 - 2\beta x_0 y - 2\eta x_0 + dx_0 + c_1y + c_2y}{c_1y + dx_0 - c_2y}$. Taking account of condition (18), it gives $\varphi(\cot \psi) > 1$, so the slow manifold does not exist.

Based on the above analysis, the plane \mathbb{R}^2 has now been divided into seven regions $G_1, G_2, G_3, I_1, I_2, I_3$, and the circle.

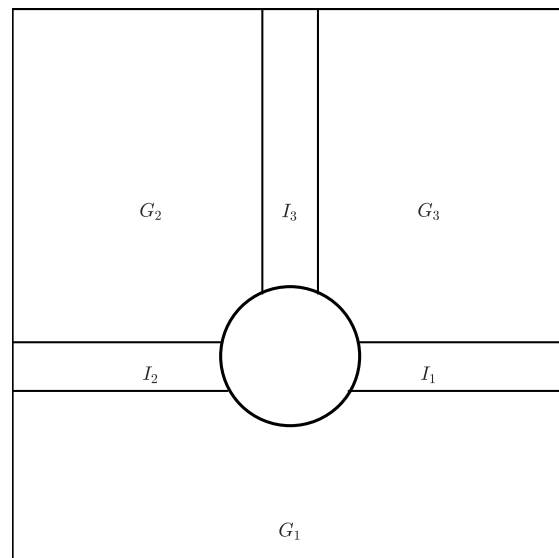


Figure 3. The blowing up and regularization approach separates \mathbb{R}^2 into seven regions $G_1, G_2, G_3, I_1, I_2, I_3$, and the circle.

Concerning the nonsmooth fold bifurcation that occurred in the Filippov system (16), after regularization, we have the following results.

Proposition 2. A saddle-node bifurcation occurs in the regularized system of (16).

Proof. An equilibrium (ordinary equilibrium, boundary equilibrium, or pseudoequilibrium) of the Filippov system Z remains an equilibrium of its regularization R_Z with the same type of stability [27]. For the three cases of the nonsmooth fold bifurcation, it is straightforward to derive the following results:

1. When $x_0 < x_1 < x_3 < x_2$ and $y_1 < y_0 < y_3 < y_2$, the stable focus in region G_3 and the center equilibrium in region G_1 are preserved, while the pseudosaddle point on Σ_{+,y_0} becomes a saddle in region I_1 after regularization;
2. When $x_0 < x_1 < x_3 < x_2$ and $y_0 = y_3$, the center equilibrium in region G_1 is preserved. After regularization, the boundary equilibrium of F_3 , $(\frac{\delta+c_2}{\beta}, y_0)$, is preserved but located at $(\frac{\delta+c_2}{\beta}, y)$, where $y_0 - \varepsilon < y < y_0 + \varepsilon$;
3. When $x_0 < x_1 < x_3 < x_2$ and $y_0 > y_3$, the regularized system R_ε only has a center equilibrium in region G_1 .

In the entire process, as y_0 varies, the center stays unchanged, while the focus and the saddle collide and then disappear. Thus, a saddle-node bifurcation occurs. \square

In the next section, we assign specific parameter values to the Filippov system (16) and its regularization, which helps us observe the difference in the dynamical behavior between the Filippov system (16) and its regularized system.

3.1.3. Simulation Results

The simulation results with the fixed parameter values $a = 1, \beta = 0.5, \eta = 0.3, \delta = 0.5, d = 0.2, c_1 = 0.6, c_2 = 0.55, x_0 = 0.6$ are shown in Figure 4. It is simple to observe that an admissible focus $(2.1, 2.94)$ collides with the pseudosaddle $(10/7, 2)$, and then both disappear, while the center equilibrium $(1, 7/5)$ remains unchanged as y_0 varies. Therefore, a nonsmooth fold bifurcation occurs.

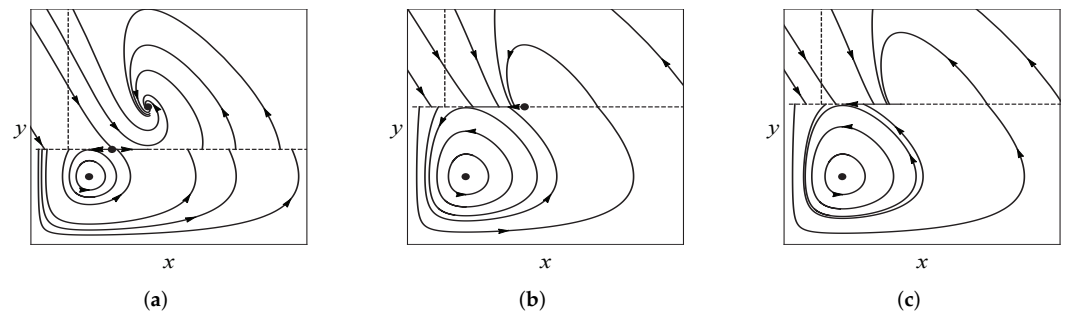


Figure 4. Nonsmooth fold bifurcation. Parameters are fixed at (a) $y_0 = 2$, (b) $y_0 = 2.94$, (c) $y_0 = 3$.

Under the chosen parameter values, the Filippov system (16) becomes

$$Z(x, y) = \begin{cases} F_1(x, y), & (x, y) \in G_1, \\ F_2(x, y), & (x, y) \in G_2, \\ F_3(x, y), & (x, y) \in G_3, \end{cases} \tag{28a}$$

where

$$\begin{aligned} F_1(x, y) &= (x - 0.5xy - 0.3x, 0.5xy - 0.5y), \\ F_2(x, y) &= (x - 0.5xy - 0.3x + 0.2x + 0.6y, 0.5xy - 0.5y - 0.6y), \\ F_3(x, y) &= (x - 0.5xy - 0.3x + 0.55y, 0.5xy - 0.5y - 0.55y). \end{aligned} \tag{28b}$$

Considering each part of the discontinuity set, we have the following results.

- *Case I.*
Compared with the analysis in Section 3.1.2, the dynamics of the singular point Σ_{x_0,y_0} can be discussed in three different regions.
For $0 < \theta < \pi/2$,

$$\theta' = \cos \theta(0.5x_0y_0 - 0.5y_0 - 0.55y_0) - \sin \theta(x_0 - 0.5x_0y_0 - 0.3x_0 + 0.55y_0);$$

For $\pi/2 < \theta < \pi$,

$$\theta' = \cos \theta(0.5x_0y_0 - 0.5y_0 - 0.6y_0) - \sin \theta(x_0 - 0.5x_0y_0 - 0.3x_0 + 0.2x_0 + 0.6y_0);$$

For $\pi < \theta < 2\pi$,

$$\theta' = \cos \theta(0.5x_0y_0 - 0.5y_0) - \sin \theta(x_0 - 0.5x_0y_0 - 0.3x_0).$$

- *Case II.*
In region I_1 , the slow manifold is given by

$$\mathcal{M}_1 = \left\{ (x, \psi) \in \mathbb{R} \times (0, \pi) : -\sin \psi \left[0.5xy_0 - 0.5y_0 - \frac{0.55y_0}{2} - \frac{0.55y_0}{2} \varphi(\cot \psi) \right] = 0 \right\},$$

which is a curve that connects $(x, \psi) = (2.1, 0)$ and $(x, \psi) = (1, \pi)$. However, the point $(1, \pi)$ is not normally hyperbolic since

$$\left. \frac{\partial}{\partial \psi} \left[-\sin \psi \left(0.5xy - 0.5y - \frac{0.55y}{2} - \frac{0.55y}{2} \varphi(\cot \psi) \right) \right] \right|_{(1,\pi)} = 0.$$

Therefore, it needs additional blow-up. First of all, this point is translated to the origin by $(x_1, \psi_1) = (x - 1, \psi - \pi)$. Then, we perform the blowing up $\psi_1 = s \sin \vartheta$, $x_1 = s \cos \vartheta$ with $s \geq 0$ and $\vartheta \in [\pi, 2\pi]$. With the new coordinates, it gives the following:

$$s' = -\sin(s \sin \vartheta + \pi) \sin \vartheta G(s, \vartheta), \quad \vartheta' = -\frac{\cos \vartheta \sin(s \sin \vartheta + \pi)}{s} G(s, \vartheta),$$

where $G(s, \vartheta) = 0.5(s \cos \vartheta + 1)y - 0.5y - \frac{0.55y}{2} - \frac{0.55y}{2} \varphi(\cot(s \sin \vartheta + \pi))$. It is easy to check that $G(0, \vartheta) = 0$ and $\frac{\partial G}{\partial s} = 0.5y \cos \vartheta$. Since $\lim_{s \rightarrow 0} \frac{\vartheta'}{s} = 0.5y \cos^2 \vartheta \sin \vartheta$, the angle component on the blowing up locus is decreasing for $\vartheta \in [\pi, 2\pi]$.

- *Case III.*
In region I_2 , the slow manifold does not exist.
- *Case IV.*
In region I_3 , the slow manifold does not exist.

Now, we look at the global dynamics of the regularized system of (28) as the parameter y_0 varies. Recall that the plane \mathbb{R}^2 has been divided into seven regions after regularization. Next, we describe the dynamics of each region. First of all, for all the cases, the dynamics of the regularized system in G_1, G_2, G_3 are defined by the dynamics of F_1, F_2, F_3 in the respective region. In region I_2 , there is no equilibrium, and the flow is smoothly connected to the flows of G_1 and G_2 . The flow in region I_3 smoothly connects to the flows of G_2 and G_3 . Subsequently, we consider the dynamics for the other regions for the three cases discussed in Proposition 3.

- For the case $y_1 < y_0 < y_3 < y_2$, choosing $y_0 = 2$ since $y_3 = 2.94$ under the chosen parameter values, from the analysis of case I, we have the following on the circle:
 1. When $0 < \theta < \pi/2$, $\theta' = -0.92 \sin \theta - 1.5 \cos \theta < 0$. Thus, θ is decreasing;

2. When $\pi/2 < \theta < \pi$, $\theta' = -1.14 \sin \theta - 1.6 \cos \theta$. Then, $\theta' < 0$ for $\pi/2 < \theta < \theta_0$, while $\theta' > 0$ for $\theta_0 < \theta < \pi$. Here θ_0 is given by $\theta'|_{\theta=\theta_0} = 0$;
3. When $\pi < \theta < 2\pi$, $\theta' = 0.18 \sin \theta - 0.4 \cos \theta$. Then, $\theta' > 0$ for $\pi < \theta < \theta_0$, while $\theta' < 0$ for $\theta_0 < \theta < 3\pi/2$, where θ_0 is defined as the same as the previous case. When $3\pi/2 < \theta < 2\pi$, $\theta' < 0$.

In region I_1 , from the analysis of case II, it is easy to compute that the reduced problem has an equilibrium at $(x, \psi) = (10/7, \psi_0)$, and $\varphi(\cot \psi_0) = -\frac{85}{385}$. The flow goes in the positive direction of the x -axis if $\psi \in (0, \psi_0)$ and in the negative direction of the x -axis if $\psi \in (\psi_0, \pi)$; see Figure 5a.

- When $y_0 = y_3 = 2.94$, on the circle, we have the following:

1. When $0 < \theta < \pi/2$, $\theta' = -1.155 \sin \theta - 2.205 \cos \theta < 0$;
2. When $\pi/2 < \theta < \pi$, $\theta' = -1.422 \sin \theta - 2.352 \cos \theta$. Then, $\theta' < 0$ for $\pi/2 < \theta < \theta_0$, while $\theta' > 0$ for $\theta_0 < \theta < \pi$, where $\theta'|_{\theta=\theta_0} = 0$;
3. When $\pi < \theta < 2\pi$, $\theta' = 0.462 \sin \theta - 0.588 \cos \theta$. Therefore, $\theta' > 0$ for $\pi < \theta < \theta_0$, while $\theta' < 0$ for $\theta_0 < \theta < 3\pi/2$. For $3\pi/2 < \theta < 2\pi$, $\theta' < 0$.

In region I_1 , the reduced problem has one equilibrium at $(x, \psi) = (2.1, 0)$. The vector points to the negative direction of the x -axis on the slow manifold.

- When $y_0 > y_3$, for instance, $y_0 = 3$, then on the circle, we have the following:

1. When $0 < \theta < \pi/2$, $\theta' = -1.17 \sin \theta - 2.25 \cos \theta < 0$;
2. When $\pi/2 < \theta < \pi$, $\theta' = -1.44 \sin \theta - 2.4 \cos \theta$. Then, $\theta' < 0$ for $\pi/2 < \theta < \theta_0$, while $\theta' > 0$ for $\theta_0 < \theta < \pi$;
3. When $\pi < \theta < 2\pi$, $\theta' = 0.48 \sin \theta - 0.6 \cos \theta$. For this case, when $\pi < \theta < 3\pi/2$, $\sin \theta < 0, \cos \theta < 0$, there is a θ_0 that $\theta' = 0$. Then, $\theta' > 0$ for $\pi < \theta < \theta_0$, while $\theta' < 0$ for $\theta_0 < \theta < 3\pi/2$. When $3\pi/2 < \theta < 2\pi$, $\sin \theta < 0, \cos \theta > 0$, we have $\theta' < 0$.

In region I_1 , the reduced problem has no equilibrium, and the vector of the slow manifold points to the negative direction of the x -axis; see Figure 5c.

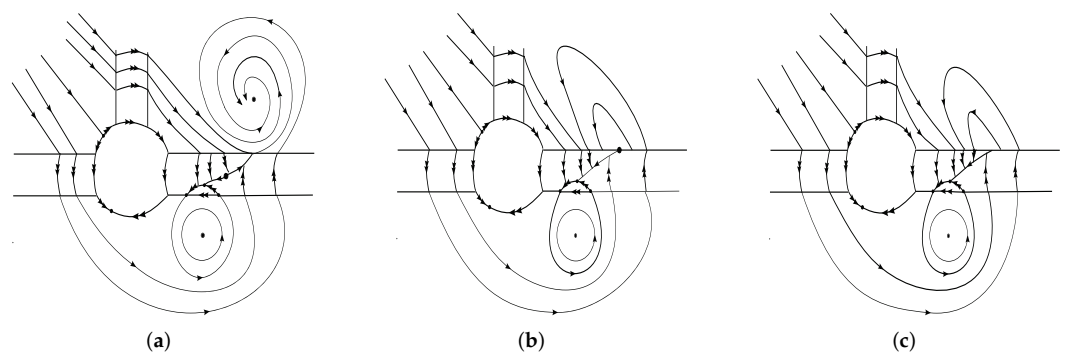


Figure 5. Phase portrait of the regularization of system (28). The semicylinder represents the blowing up locus and the flows with a simple arrow and with a double arrow represent the slow and fast systems, respectively. Generated by (a) $y_0 = 2$, (b) $y_0 = 2.94$, (c) $y_0 = 3$.

3.2. The Filippov Avian-Only Model

Influenza is the most diversified in birds, particularly in wild waterfowl. Outbreaks of avian influenza in domestic poultry could, through a process of genetic reassortment, mutation, or both, introduce new influenza subtypes into the human population. In the context

of widespread susceptibility, such an event could be the precursor of a pandemic. Since there is no cure for avian influenza, recommendations for precautions are both necessary and reasonable during poultry outbreaks. Many different types of mathematical models have been proposed for comparing interventions aimed at preventing and controlling an influenza pandemic [48–50]. Among all the preventative strategies, they have found that culling infected birds and those in contact with them is an effective method to control the spread [12,16,51]. Recently, an avian-only model has been constructed that incorporates culling only the infected birds, or both the infected and susceptible birds, depending on whether the numbers of infected and susceptible birds exceed the economic threshold values or not. The specific rules are as follows:

1. When $y < y_0$, no control strategy is taken;
2. When $y > y_0, x < x_0$, infected birds are culled at a rate of c_2 ;
3. When $y > y_0, x > x_0$, infected birds are culled at a rate of c_3 and, meanwhile, susceptible birds are culled at a rate of c_1 ,

Therefore, an avian-only model can be described by the following Filippov system:

$$Z(X) = \begin{cases} F_1(X), & \text{if } X \in G_1, \\ F_2(X), & \text{if } X \in G_2, \\ F_3(X), & \text{if } X \in G_3, \end{cases} \tag{29a}$$

with

$$\begin{aligned} F_1(x, y) &= \left(rx \left(1 - \frac{x}{K} \right) - \beta xy, \beta xy - \mu y - dy \right), \\ F_2(x, y) &= \left(rx \left(1 - \frac{x}{K} \right) - \beta xy, \beta xy - \mu y - dy - c_2 y \right), \\ F_3(x, y) &= \left(rx \left(1 - \frac{x}{K} \right) - \beta xy - c_1 x, \beta xy - \mu y - dy - c_3 y \right), \end{aligned} \tag{29b}$$

in regions

$$G_1 = \{(x, y) | y < y_0\}, G_2 = \{(x, y) | x < x_0, y > y_0\}, G_3 = \{(x, y) | x > x_0, y > y_0\}. \tag{29c}$$

The discontinuity set $\Sigma = \Sigma_1 \cup \Sigma_2$ is defined the same as in Section 3.1, where

$$\Sigma_1 = \{X \in \mathbb{R}^2 : y - y_0 = 0\}, \quad \Sigma_2 = \{X \in \mathbb{R}^2 : x - x_0 = 0, y - y_0 \geq 0\}.$$

Here, x and y represent the numbers of susceptible and infected birds. $\beta > 0$ denotes the transmission rate. $\mu > 0$ is the natural death rate. $d > 0$ is the disease-related death rate. Notice that the susceptible birds are assumed to be subject to logistic growth, where r is the intrinsic growth rate and K is the maximal carrying capacity. $x_0, y_0 > 0$ denote the respective susceptible threshold value and the infected threshold level. $r > c_1, c_2 < c_3$ and $c_1, c_2, c_3 > 0$.

3.2.1. Equilibria and Bifurcation

System (29) in region G_i has two types of equilibria: the disease-free equilibria E_{i0}^1, E_{i0}^2 and the endemic equilibrium $E_i, i = 1, 2, 3$, which can be expressed as

$$\begin{aligned}
 E_{10}^1 &= (0, 0), & E_{10}^2 &= (K, 0), \\
 E_1 &= (x_1, y_1) = \left(\frac{\mu + d}{\beta}, \frac{1}{\beta} \left(r - \frac{r(\mu + d)}{K\beta} \right) \right); \\
 E_{20}^1 &= (0, 0), & E_{20}^2 &= (K, 0), \\
 E_2 &= (x_2, y_2) = \left(\frac{\mu + d + c_2}{\beta}, \frac{1}{\beta} \left(r - \frac{r(\mu + d + c_2)}{K\beta} \right) \right); \\
 E_{30}^1 &= (0, 0), & E_{30}^2 &= (K, 0), \\
 E_3 &= (x_3, y_3) = \left(\frac{\mu + d + c_3}{\beta}, \frac{1}{\beta} \left(r - c_1 - \frac{r(\mu + d + c_3)}{K\beta} \right) \right).
 \end{aligned}$$

In [16], they discuss the stability of all the equilibria of 16 different cases depending on the values of x_i and $y_i, i = 0, 1, 2, 3$. In this work, we only concentrate on the bifurcation analysis of the case

$$\begin{aligned}
 x_1 < x_2 < x_3 < x_0 \quad \text{with} \quad y_0 < y_3 < y_2 < y_1, \quad \text{or} \quad y_3 < y_0 < y_2 < y_1, \\
 \text{or} \quad y_3 < y_2 < y_0 < y_1, \quad \text{or} \quad y_3 < y_2 < y_1 < y_0.
 \end{aligned} \tag{30}$$

The other cases are similar, so we omit their analysis here. Moreover, in this paper, we only discuss the case when the unique endemic equilibrium E_i exists. Then, the disease-free equilibrium E_{i0}^1 is always unstable, while the equilibrium E_i in region G_i is globally asymptotically stable, $i = 1, 2, 3$.

Besides, for our analysis, the condition

$$\frac{r}{\beta} \left(1 - \frac{x_0}{K} \right) < y_0 \tag{31}$$

is imposed.

Proposition 3. *A persistence bifurcation occurs in system (29) under the condition $x_1 < x_2 < x_3 < x_0$. Specifically, the following holds:*

1. When $x_1 < x_2 < x_3 < x_0$ and $y_0 < y_2$, system (29) has a stable focus;
2. When $x_1 < x_2 < x_3 < x_0$ and $y_0 = y_2$, this focus turns into a boundary equilibrium;
3. When $x_1 < x_2 < x_3 < x_0$ and $y_3 < y_2 < y_0 < y_1$, the boundary equilibrium turns into a pseudonode.

The proof of the existence and stability of each equilibrium is derived from the work in [16,52], and the proof of this proposition can directly be derived from it.

Next, we study the regularization of the avian-only system (29).

3.2.2. Regularization

Again, the discontinuity set Σ of system (29) can be divided into the simple discontinuity $\Sigma_{+,y_0} \cup \Sigma_{-,y_0} \cup \Sigma_{x_0,+}$ and the nonsimple discontinuity Σ_{x_0,y_0} . Subsequently, the regularization method is applied separately to each part of the discontinuity set of the Filippov avian-only model (29).

- *Case I.*

For the nonsimple discontinuity Σ_{x_0,y_0} , it is firstly transformed into a simple discontinuity by the map (19). Then, the dynamics are given by

$$\theta' = -f_i \sin \theta + g_i \cos \theta, \quad F_i = (f_i, g_i), \quad i = 1, 2, 3.$$

For $0 < \theta < \pi/2$, $F_3(x, y) = \left(rx\left(1 - \frac{x}{K}\right) - \beta xy - c_1x, \beta xy - \mu y - dy - c_3y \right)$, the dynamics are given by

$$\theta' = \cos \theta(\beta x_0 y_0 - \mu y_0 - dy_0 - c_3 y_0) - \sin \theta \left(rx_0 \left(1 - \frac{x_0}{K} \right) - \beta x_0 y_0 - c_1 x_0 \right);$$

For $\pi/2 < \theta < \pi$, $F_2(x, y) = \left(rx\left(1 - \frac{x}{K}\right) - \beta xy, \beta xy - \mu y - dy - c_2y \right)$, the dynamics is

$$\theta' = \cos \theta(\beta x_0 y_0 - \mu y_0 - dy_0 - c_2 y_0) - \sin \theta \left(rx_0 \left(1 - \frac{x_0}{K} \right) - \beta x_0 y_0 \right);$$

For $\pi < \theta < 2\pi$, $F_1(x, y) = \left(rx\left(1 - \frac{x}{K}\right) - \beta xy, \beta xy - \mu y - dy \right)$, the dynamics are

$$\theta' = \cos \theta(\beta x_0 y_0 - \mu y_0 - dy_0) - \sin \theta \left(rx_0 \left(1 - \frac{x_0}{K} \right) - \beta x_0 y_0 \right).$$

Now, we apply the regularization method to the other boundaries.

- *Case II.*

For the Filippov system

$$Z_1(x, y) = \begin{cases} F_1(x, y), & (x, y) \in G_1, \\ F_3(x, y), & (x, y) \in G_3, \end{cases}$$

with the boundary $\Sigma_{+,y_0} = \{(x, y_0) | y = y_0, x > x_0\}$, the regularized vector field is

$$R_{Z_1} = \left[\frac{1}{2} + \frac{1}{2} \varphi \left(\frac{y - y_0}{\varepsilon} \right) \right] F_3(x, y) + \left[\frac{1}{2} - \frac{1}{2} \varphi \left(\frac{y - y_0}{\varepsilon} \right) \right] F_1(x, y). \tag{32}$$

Around region Σ_{+,y_0} , the differential system is given by

$$\begin{aligned} \dot{x} &= \left[\frac{1}{2} + \frac{1}{2} \varphi \left(\frac{y - y_0}{\varepsilon} \right) \right] \left(rx \left(1 - \frac{x}{K} \right) - \beta xy - c_1x \right) - \left[\frac{1}{2} - \frac{1}{2} \varphi \left(\frac{y - y_0}{\varepsilon} \right) \right] \beta xy \\ &\quad + \left[\frac{1}{2} - \frac{1}{2} \varphi \left(\frac{y - y_0}{\varepsilon} \right) \right] rx \left(1 - \frac{x}{K} \right) \\ &= rx \left(1 - \frac{x}{K} \right) - \beta xy - \frac{c_1x}{2} - \frac{c_1x}{2} \varphi \left(\frac{y - y_0}{\varepsilon} \right), \\ \dot{y} &= \left[\frac{1}{2} + \frac{1}{2} \varphi \left(\frac{y - y_0}{\varepsilon} \right) \right] (\beta xy - \mu y - dy - c_3y) + \left[\frac{1}{2} - \frac{1}{2} \varphi \left(\frac{y - y_0}{\varepsilon} \right) \right] (\beta xy - \mu y) \\ &\quad - \left[\frac{1}{2} - \frac{1}{2} \varphi \left(\frac{y - y_0}{\varepsilon} \right) \right] dy \\ &= \beta xy - \mu y - dy - \frac{c_3y}{2} - \frac{c_3y}{2} \varphi \left(\frac{y - y_0}{\varepsilon} \right). \end{aligned} \tag{33}$$

Then, system (33) can be transformed into a singular perturbation problem by

$$y = y_0 + \eta \cos \psi, \quad \varepsilon = \eta \sin \psi, \tag{34}$$

where $\eta \geq 0$ and $\psi \in [0, \pi]$, which is

$$\begin{aligned} \eta \dot{\psi} &= -\sin \psi \left[\beta x(y_0 + \eta \cos \psi) - \mu(y_0 + \eta \cos \psi) - d(y_0 + \eta \cos \psi) - \frac{c_3 y_0}{2} \right. \\ &\quad \left. - \frac{c_3 \eta \cos \psi}{2} - \frac{c_3(y_0 + \eta \cos \psi)}{2} \varphi(\cot \psi) \right], \\ \dot{x} &= rx \left(1 - \frac{x}{K} \right) - \beta x(y_0 + \eta \cos \psi) - \frac{c_1x}{2} + \frac{c_1x}{2} \varphi(\cot \psi). \end{aligned}$$

Now, $\varepsilon = 0$ is represented by $\eta = 0$. The slow manifold is given by $\mathcal{M}_1 = \left\{ (x, \psi) \in \mathbb{R} \times (0, \pi) : -\sin \psi \left[\beta xy_0 - \mu y_0 - dy_0 - \frac{c_3}{2} y_0 - \frac{\varphi(\cot \psi)}{2} c_3 y_0 \right] = 0 \right\}$, i.e., $\varphi(\cot \psi) = \frac{2\beta xy_0 - 2\mu y_0 - 2dy_0 - c_3 y_0}{c_3 y_0} = \frac{2\beta x - 2\mu - 2d - c_3}{c_3}$. Since $x > x_0 > x_3 = \frac{\mu + d + c_3}{\beta}$, $\varphi(\cot \psi) > 1$, there is no slow manifold.

- **Case III.**
For the Filippov system

$$Z_2(x, y) = \begin{cases} F_1(x, y), & (x, y) \in G_1, \\ F_2(x, y), & (x, y) \in G_2, \end{cases}$$

with the boundary $\Sigma_{-,y_0} = \{(x, y_0) | y = y_0, x < x_0\}$, the regularized system is

$$R_{Z_2} = \left[\frac{1}{2} + \frac{1}{2} \varphi \left(\frac{y - y_0}{\varepsilon} \right) \right] F_2(x, y) + \left[\frac{1}{2} - \frac{1}{2} \varphi \left(\frac{y - y_0}{\varepsilon} \right) \right] F_1(x, y). \tag{35}$$

Around region Σ_{-,y_0} , the differential system is given by

$$\begin{aligned} \dot{x} &= rx \left(1 - \frac{x}{K} \right) - \beta xy, \\ \dot{y} &= \beta xy - \mu y - dy - \frac{c_2 y}{2} - \frac{c_2 y}{2} \varphi \left(\frac{y - y_0}{\varepsilon} \right). \end{aligned} \tag{36}$$

Applying the transformation (34), we obtain

$$\begin{aligned} \eta \dot{\psi} &= -\sin \psi \left[\beta x(y_0 + \eta \cos \psi) - \mu(y_0 + \eta \cos \psi) - d(y_0 + \eta \cos \psi) - \frac{c_2 y_0}{2} \right. \\ &\quad \left. + \frac{c_2 \eta \cos \psi}{2} - \frac{c_2(y_0 + \eta \cos \psi)}{2} \varphi(\cot \psi) \right], \\ \dot{x} &= rx \left(1 - \frac{x}{K} \right) - \beta x(y_0 + \eta \cos \psi). \end{aligned}$$

For $\varepsilon = 0$, the slow manifold is

$$\mathcal{M}_2 = \left\{ (x, \psi) \in \mathbb{R} \times (0, \pi) : -\sin \psi \left[\beta xy_0 - \mu y_0 - dy_0 - \frac{c_2 y_0}{2} - \varphi(\cot \psi) \frac{c_2 y_0}{2} \right] = 0 \right\},$$

i.e., $\alpha(\cot \psi) = \frac{2\beta x - 2\mu - 2d - c_2}{c_2}$. The slow manifold is a curve that connects $(x, \psi) = \left(\frac{\mu + d + c_2}{\beta}, 0 \right)$ and $(x, \psi) = \left(\frac{\mu + d}{\beta}, \pi \right)$.

- **Case IV.**
For the Filippov system

$$Z_3(x, y) = \begin{cases} F_2(x, y), & (x, y) \in G_2, \\ F_3(x, y), & (x, y) \in G_3, \end{cases}$$

with the boundary $\Sigma_{x_0,+} = \{(x_0, y) | x = x_0, y > y_0\}$, its regularized system is

$$R_{Z_3} = \left[\frac{1}{2} + \frac{1}{2} \varphi \left(\frac{x - x_0}{\varepsilon} \right) \right] F_3(x, y) + \left[\frac{1}{2} - \frac{1}{2} \varphi \left(\frac{x - x_0}{\varepsilon} \right) \right] F_2(x, y). \tag{37}$$

Around region $\Sigma_{x_0,+}$, the differential system is given by

$$\begin{aligned} \dot{x} &= rx \left(1 - \frac{x}{K} \right) - \beta xy - \frac{c_1 x}{2} - \frac{c_1 x}{2} \varphi \left(\frac{x - x_0}{\varepsilon} \right), \\ \dot{y} &= \beta xy - \mu y - dy - \frac{c_2 y + c_3 y}{2} + \frac{c_2 y - c_3 y}{2} \varphi \left(\frac{x - x_0}{\varepsilon} \right). \end{aligned} \tag{38}$$

Then, system (38) is transformed into a singular perturbation problem by map (27) as

$$\begin{aligned} \eta \dot{\psi} &= -\sin \psi \left[r(x_0 + \eta \cos \psi) \left(1 - \frac{x_0 + \eta \cos \psi}{K} \right) - \beta(x_0 + \eta \cos \psi)y - \frac{c_1 x_0}{2} \right. \\ &\quad \left. - \frac{c_1 \eta \cos \psi}{2} - \frac{c_1(x_0 + \eta \cos \psi)}{2} \varphi(\cot \psi) \right], \\ \dot{y} &= \beta(x_0 + \eta \cos \psi)y - \mu y - dy - \frac{c_2 y + c_3 y}{2} + \frac{c_2 y - c_3 y}{2} \varphi(\cot \psi). \end{aligned}$$

For $\varepsilon = 0$, the slow manifold is given by

$$\begin{aligned} \mathcal{M}_3 &= \left\{ (\psi, y) \in (0, \pi) \times \mathbb{R} : -\sin \psi \left(r x_0 \left(1 - \frac{x_0}{K} \right) - \beta x_0 y - \frac{c_1 x_0}{2} - \frac{c_1 x_0}{2} \varphi(\cot \psi) \right) = 0 \right\}, \\ \text{i.e., } \varphi(\cot \psi) &= \frac{2 \left(r x_0 \left(1 - \frac{x_0}{K} \right) - \beta x_0 y \right) - c_1 x_0}{c_1 x_0} = \frac{2 \left(r \left(1 - \frac{x_0}{K} \right) - \beta y \right) - c_1}{c_1}. \end{aligned}$$

Taking account of the condition (31) and $y > y_0$, it gives $\varphi(\cot \psi) < -1$. There is no slow manifold.

Considering persistence bifurcation happened in the Filippov system (29), after regularization, we have the following conclusion.

Proposition 4. Persistence bifurcation disappears after regularization.

Proof. Since the quantity and stability of the equilibria of Z do not change after regularization, it is straightforward to derive the following results:

1. When $x_1 < x_2 < x_3 < x_0$ and $y_0 < y_2$, the stable focus in region G_2 preserves after regularization;
2. When $x_1 < x_2 < x_3 < x_0$ and $y_0 = y_2$, after regularization, the boundary equilibrium of $F_2 \left(\frac{\mu+d+c_2}{\beta}, y_0 \right)$ is preserved but located at $\left(\frac{\mu+d+c_2}{\beta}, y \right)$, where $y_0 - \varepsilon < y < y_0 + \varepsilon$;
3. When $x_1 < x_2 < x_3 < x_0$ and $y_3 < y_2 < y_0 < y_1$, the regularized system R_Z has a stable node in region I_2 .

In the entire process, as y_0 varies, the regularized system R_Z always has a stable equilibrium but is located at different regions. Besides, it is simple to check that system R_Z has no other equilibria. Since no qualitative property changes as the parameter y_0 varies, there is no bifurcation occurring in system R_Z . □

In the next section, we fix specific parameter values to observe the persistence bifurcation and its qualitative properties after regularization.

3.2.3. Simulation Results

The simulation results are given in Figure 6 when the parameter values are fixed as $r = 0.0047, \beta = 2 \times 10^{-5}, K = 600, \mu = 1.2 \times 10^{-3}, d = 4 \times 10^{-3}, c_1 = 0.001, c_2 = 0.003, c_3 = 0.006, x_0 = 570$. It is simple to observe from Figure 6 that an admissible focus (410, 74.416) turns into a pseudonode (344.68, 100) as y_0 varies, while no extra equilibria appear. Therefore, a persistence bifurcation occurs in system (29).

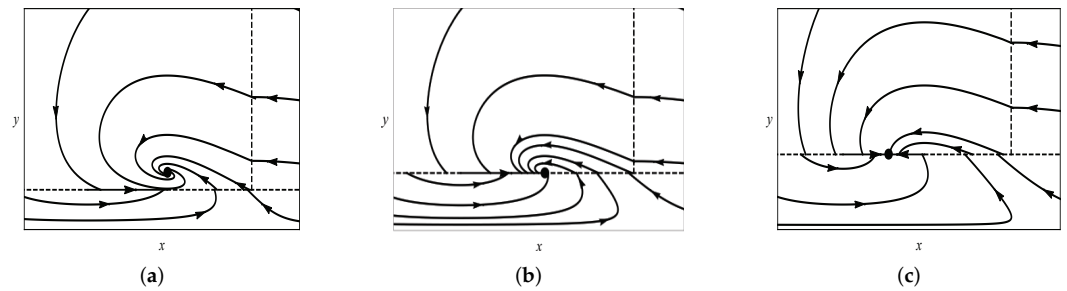


Figure 6. Persistence bifurcation. Generated by (a) $y_0 = 50$, (b) $y_0 = y_2$, (c) $y_0 = 100$.

Now, we look at what happens to this bifurcation after regularization. Under the chosen parameter values, the Filippov system (29) becomes

$$Z(x, y) = \begin{cases} F_1(x, y), & (x, y) \in G_1, \\ F_2(x, y), & (x, y) \in G_2, \\ F_3(x, y), & (x, y) \in G_3, \end{cases} \tag{39a}$$

where

$$\begin{aligned} F_1(x, y) &= \left(0.0047x \left(1 - \frac{x}{600}\right) - 2 \times 10^{-5}xy, 2 \times 10^{-5}xy - 1.2 \times 10^{-3}y - 4 \times 10^{-3}y\right), \\ F_2(x, y) &= \left(0.0047x \left(1 - \frac{x}{600}\right) - 2 \times 10^{-5}xy, 2 \times 10^{-5}xy - 1.2 \times 10^{-3}y - 4 \times 10^{-3}y - 0.003y\right), \\ F_3(x, y) &= \left(0.0047x \left(1 - \frac{x}{600}\right) - 2 \times 10^{-5}xy - 0.001x, 2 \times 10^{-5}xy - 1.2 \times 10^{-3}y - 4 \times 10^{-3}y - 0.006y\right). \end{aligned} \tag{39b}$$

Considering each part of the discontinuity set, we have the following results.

- **Case I.** Compared with the analysis in Section 3.1.2, the dynamics of Σ_{x_0, y_0} can be discussed in three different regions. For $0 < \theta < \pi/2$,

$$\theta' = \cos \theta (2 \times 10^{-5}x_0y_0 - 1.2 \times 10^{-3}y_0 - 4 \times 10^{-3}y_0 - 0.006y_0) - \sin \theta \left(0.0047x_0 \left(1 - \frac{x_0}{600}\right) - 2 \times 10^{-5}x_0y_0 - 0.001x_0\right);$$

For $\pi/2 < \theta < \pi$,

$$\theta' = \cos \theta (2 \times 10^{-5}x_0y_0 - 1.2 \times 10^{-3}y_0 - 4 \times 10^{-3}y_0 - 0.003y_0) - \sin \theta \left(0.0047x_0 \left(1 - \frac{x_0}{600}\right) - 2 \times 10^{-5}x_0y_0\right);$$

For $\pi < \theta < 2\pi$,

$$\theta' = \cos \theta (2 \times 10^{-5}x_0y_0 - 1.2 \times 10^{-3}y_0 - 4 \times 10^{-3}y_0) - \sin \theta (0.0047x_0 \left(1 - \frac{x_0}{600}\right) - 2 \times 10^{-5}x_0y_0).$$

- **Case II.** In region I_1 , the slow manifold is an empty set for this case.
- **Case III.**

In region I_2 , the slow manifold is $\mathcal{M}_2 = \{(x, \psi) \in \mathbb{R} \times (0, \pi) : u(x, \psi) = 0\}$, where $u(x, \psi) = -\sin \psi \left[2 \times 10^{-5}xy_0 - 1.2 \times 10^{-3}y_0 - 4 \times 10^{-3}y_0 - \frac{0.003y_0}{2} - \frac{0.003y_0}{2}\varphi(\cot \psi) \right]$. It is a curve connecting the points $(x, \psi) = (260, \pi)$ and $(x, \psi) = (410, 0)$.

Notice that the point $(260, \pi)$ is not normally hyperbolic since

$$\left. \frac{\partial u(x, \psi)}{\partial \psi} \right|_{(260, \pi)} = 0.$$

Therefore, it needs additional blow-up. First of all, we translate this point to the origin with $(x_2, \psi_2) = (x - 260, \psi - \pi)$. Next, the blowing up $\psi_2 = s \sin \vartheta, x_2 = s \cos \vartheta$ with $s \geq 0$ and $\vartheta \in [\pi, 2\pi]$ is performed to this point. With new coordinates, it gives

$$s' = -\sin(s \sin \vartheta + \pi) \sin \vartheta G(s, \vartheta), \quad \vartheta' = -\frac{\cos \vartheta \sin(s \sin \vartheta + \pi)}{s} G(s, \vartheta),$$

where $G(s, \vartheta) = 2 \times 10^{-5}(s \cos \vartheta + 260)y_0 - 1.2 \times 10^{-3}y_0 - 4 \times 10^{-3}y_0 - \frac{0.003y_0}{2} - \frac{0.003y_0}{2}\varphi(\cot(s \sin \vartheta + \pi))$. One verifies that $G(0, \vartheta) = 0$ and $\frac{\partial G}{\partial s} = 2 \times 10^{-5}y_0 \cos \vartheta$.

Thus, $\lim_{s \rightarrow 0} \frac{\vartheta'}{s} = 2 \times 10^{-5}y_0 \cos^2 \vartheta \sin \vartheta$. This means that the angle component is decreasing for $\vartheta \in [\pi, 2\pi]$.

- *Case IV.*

In region I_3 , the slow manifold is an empty set.

Now, we look at the global dynamics of the regularized system of (39) as the parameter y_0 varies. The dynamics of R_Z in G_1, G_2, G_3 are defined by the dynamics of F_1, F_2, F_3 in the respective region. In region I_1 , there is no equilibrium, and the flow is continuously connected to the flows of G_1 and G_3 . The flow in region I_3 continuously connects to the flows of G_2 and G_3 . Subsequently, we look at the dynamics in the other regions for the three cases discussed in Proposition 4.

- For the case $y_0 < y_2$, considering $y_0 = 50$ since $y_2 = 74.416$ under the chosen parameter values, from the analysis of case I, on the circle, the following holds:
 1. When $0 < \theta < \pi/2, \theta' = 1.00605 \sin \theta + 0.01 \cos \theta > 0$;
 2. When $\pi/2 < \theta < \pi, \theta' = 1.00605 \sin \theta + 0.16 \cos \theta$. For this case, there exists a θ_0 such that $\theta' = 0$. Therefore, $\theta' > 0$ for $\pi/2 < \theta < \theta_0$, while $\theta' < 0$ for $\theta_0 < \theta < \pi$;
 3. When $\pi < \theta < 2\pi, \theta' = 1.00606 \sin \theta + 0.31 \cos \theta$. Thus, $\theta' < 0$ for $\pi < \theta < 3\pi/2$ and $3\pi/2 < \theta < \theta_0$, while $\theta' > 0$ for $\theta_0 < \theta < 2\pi$, where θ_0 has the same definition as the previous case.

In region I_2 , the reduced flow goes in the positive direction of the x -axis; see Figure 7a.

- When $y_0 = y_2 = 74.416$, on the circle, the following holds:
 1. When $0 < \theta < \pi/2, \theta' = 1.28 \sin \theta + 0.015 \cos \theta > 0$;
 2. When $\pi/2 < \theta < \pi, \theta' = 0.71 \sin \theta + 0.23 \cos \theta$. Then $\theta' > 0$ for $\pi/2 < \theta < \theta_0$, while $\theta' < 0$ for $\theta_0 < \theta < \pi$, where $\theta'|_{\theta=\theta_0} = 0$;
 3. When $\pi < \theta < 2\pi, \theta' = 0.71 \sin \theta + 0.46 \cos \theta$. Thus, $\theta' < 0$ for $\pi < \theta < 3\pi/2$ and $3\pi/2 < \theta < \theta_0$, while $\theta' > 0$ for $\theta_0 < \theta < 2\pi$.

In region I_2 , the reduced problem has an equilibrium at $(x, \psi) = (410, 0)$. The flow goes in the positive direction of the x -axis; see Figure 7b.

- When $y_3 < y_2 < y_0 < y_1$, for instance, $y_0 = 100$, then on the circle, the following holds:
 1. When $0 < \theta < \pi/2, \theta' = 1.57 \sin \theta + 0.02 \cos \theta > 0$;

2. When $\pi/2 < \theta < \pi$, $\theta' = 1.006 \sin \theta + 0.32 \cos \theta$. Then, $\theta' > 0$ for $\pi/2 < \theta < \theta_0$, while $\theta' < 0$ for $\theta_0 < \theta < \pi$;
3. When $\pi < \theta < 2\pi$, $\theta' = 1.006 \sin \theta + 0.62 \cos \theta$. Thus, $\theta' < 0$ for $\pi < \theta < 3\pi/2$ and $3\pi/2 < \theta < \theta_0$, while $\theta' > 0$ for $\theta_0 < \theta < 2\pi$.

In region I_2 , the reduced problem has an equilibrium at $(x, \psi) = (344.68, \psi_0)$, and $\varphi(\cot \psi_0) = \frac{242}{1875}$, and the flow goes in the positive direction of the x -axis if $\psi \in (\psi_0, \pi)$ and goes in the negative direction of the x -axis if $\psi \in (0, \psi_0)$; see Figure 7c.

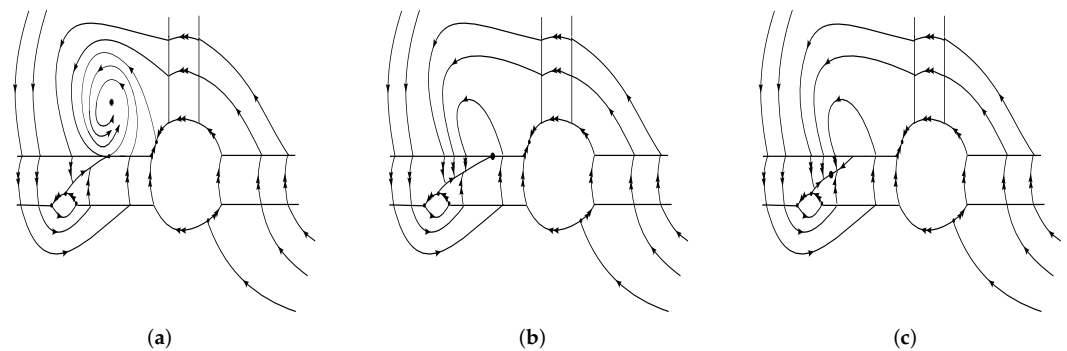


Figure 7. Phase portraits of the regularized system R_Z . Generated by (a) $y_0 = 50$, (b) $y_0 = y_2 = 74.416$, (c) $y_0 = 100$.

4. Conclusions and Future Work

In this paper, we apply the regularization approach to the Filippov system with rich discontinuity boundaries. This type of system appears in applications of various natures: control theory, classical electromagnetism theory, and relay feedback systems. Two specific examples of such types of systems are investigated in this work. We discuss the bifurcations of these systems and the corresponding ones after regularization. The nonsmooth fold bifurcation that occurs in the plant disease model becomes a saddle-node bifurcation. The persistence bifurcation happening in the Filippov avian-only model disappears after regularization. During the regularization process, the singular perturbation theory and the blow-up technique play an important role.

A further extension of this work is to investigate the more complicated bifurcations of such types of Filippov systems by regularization approach, such as the bifurcations involving limit cycles.

Author Contributions: Conceptualization, X.L. and N.C.; methodology, X.L.; software, Y.Z. and N.C.; validation, X.L., Y.Z. and N.C.; formal analysis, X.L. and Y.Z.; investigation, X.L., Y.Z. and N.C.; resources, X.L.; data curation, N.C.; writing—original draft preparation, Y.Z.; writing—review and editing, X.L. and N.C.; visualization, X.L., Y.Z. and N.C.; supervision, X.L. and N.C.; funding acquisition, X.L. All authors have read and agreed to the published version of the manuscript.

Funding: This research was funded by the Natural Science Foundation of Hebei Province of China grant number A2019403169.

Data Availability Statement: Data are contained within the article.

Conflicts of Interest: The authors declare no conflicts of interest.

References

1. Bernardo, M.D.; Budd, C.J.; Champneys, A.R.; Kowalczyk, P. *Piecewise-Smooth Dynamical Systems: Theory and Applications*, 1st ed.; Springer: Berlin/Heidelberg, Germany, 2008.
2. Bernardo, M.D.; Pagano, D.J.; Ponce, E. Non-hyperbolic Boundary Equilibrium Bifurcations in Planar Filippov Systems: A Case Study Approach. *Int. J. Bifurc. Chaos* **2008**, *18*, 1377–1392. [[CrossRef](#)]

3. Biák, M.; Hanus, T.; Janovská, D. Some applications of Filippov's dynamical systems. *J. Comput. Appl. Math.* **2013**, *254*, 132–143. [[CrossRef](#)]
4. Goh, B.S. Stability in Models of Mutualism. *Am. Nat.* **1979**, *113*, 261–275. [[CrossRef](#)]
5. Liu, L.R.; Xiang, C.C.; Tang, G.Y. Dynamics Analysis of Periodically Forced Filippov Holling II Prey-Predator Model With Integrated Pest Control. *IEEE Access* **2019**, *7*, 113889–113900. [[CrossRef](#)]
6. Qin, W.J.; Tan, X.W.; Shi, X.T.; Chen, J.H.; Liu, X.Z. Dynamics and Bifurcation Analysis of a Filippov Predator-Prey Ecosystem in a Seasonally Fluctuating Environment. *Int. J. Bifurc. Chaos* **2019**, *29*, 1–16. [[CrossRef](#)]
7. Filippov, A.F. *Differential Equations with Discontinuous Righthand Sides*, 1st ed.; Springer: Dordrecht, The Netherlands, 1988.
8. Agrawal, J.; Moudgalya, K.M.; Pani, A.K. Sliding motion of discontinuous dynamical systems described by semi-implicit index one differential algebraic equations. *Chem. Eng. Sci.* **2006**, *61*, 4722–4731. [[CrossRef](#)]
9. Chen, F.D. Permanence of periodic Holling type Predator-Prey system with stage structure for prey. *Appl. Math. Comput.* **2006**, *182*, 1849–1860. [[CrossRef](#)]
10. Chen, L.J.; Chen, F.D.; Chen, L.J. Qualitative analysis of a predator-prey model with Holling type II functional response incorporating a constant prey refuge. *Nonlinear Anal. Real World Appl.* **2010**, *11*, 246–252. [[CrossRef](#)]
11. Buzzi, C.A.; Silva, P.R.; Teixeira, M.A. Slow-fast systems on algebraic varieties bordering piecewise-smooth dynamical systems. *Bull. Sci.* **2012**, *136*, 444–462. [[CrossRef](#)]
12. Chong, N.; Smith, R. Modeling avian influenza using Filippov systems to determine culling of infected birds and quarantine. *Nonlinear Anal. Real World Appl.* **2015**, *24*, 196–218. [[CrossRef](#)]
13. Huang, L.H.; Ma, H.L.; Wang, J.F.; Huang, C.X. Global dynamics of a Filippov plant disease model with an economic threshold of infected-susceptible ratio. *J. Appl. Anal. Comput.* **2020**, *10*, 2263–2277. [[CrossRef](#)]
14. Teixeira, M.A.; Silva, P.R. Regularization and singular perturbation techniques for non-smooth systems. *Phys. Nonlinear Phenom.* **2012**, *241*, 1948–1955. [[CrossRef](#)]
15. Chen, C.; Chen, X. Rich Sliding Motion and Dynamics in a Filippov Plant-Disease System. *Int. J. Bifurc. Chaos* **2018**, *28*, 1850012. [[CrossRef](#)]
16. Yang, Y.P.; Wang, L.J. Global Dynamics and Rich Sliding Motion in an Avian-Only Filippov System in Combating Avian Influenza. *Int. J. Bifurc. Chaos* **2020**, *30*, 2050008. [[CrossRef](#)]
17. Cao, N.B.; Zhang, Y.; Liu, X. Dynamics and Bifurcations in Filippov Type of Competitive and Symbiosis Systems. *Int. J. Bifurc. Chaos* **2022**, *32*, 1–21. [[CrossRef](#)]
18. Dercole, F.; Rossa, F.D.; Colombo, A.; Kuznetsov, Y.A. Two Degenerate Boundary Equilibrium Bifurcations in Planar Filippov Systems. *SIAM J. Appl. Dyn. Syst.* **2011**, *10*, 1525–1553. [[CrossRef](#)]
19. Efstathiou, K.; Liu, X.; Broer, H.W. The Boundary-Hopf-Fold Bifurcation in Filippov Systems. *SIAM J. Appl. Dyn. Syst.* **2015**, *14*, 914–941. [[CrossRef](#)]
20. Kuznetsov, Y. A.; Rinaldi, S.; Gragnani, A. One-Parameter Bifurcations in Planar Filippov Systems. *Int. J. Bifurc. Chaos* **2003**, *13*, 1–50. [[CrossRef](#)]
21. Jelbart, S.; Kristiansen, K.U.; Wechselberger, M. Singularly Perturbed Boundary-Equilibrium Bifurcations. *Nonlinearity* **2021**, *34*, 7371–7414. [[CrossRef](#)]
22. Jelbart, S.; Kristiansen, K.U.; Wechselberger, M. Singularly Perturbed Boundary-Focus Bifurcations. *J. Differ. Equ.* **2021**, *296*, 412–492. [[CrossRef](#)]
23. Kaklamanos, P.; Kristiansen, K.U. Regularization and Geometry of Piece-wise Smooth Systems with Intersecting Discontinuity Sets. *SIAM J. Appl. Dyn. Syst.* **2019**, *18*, 1225–1264. [[CrossRef](#)]
24. Leine, R.I.; Nijmeijer, H. *Dynamics and Bifurcations of Non-Smooth Mechanical Systems*, 1st ed.; Springer: Berlin/Heidelberg, Germany, 2004.
25. Lin, Q.F. Dynamic behaviors of a commensal symbiosis model with non-monotonic functional response and non-selective harvesting in a partial closure. *Commun. Math. Biol. Neurosci.* **2018**, *2018*, 1–15.
26. Liu, X. The Discontinuous Hopf-Transversal System and Its Geometric Regularization. Ph.D. Thesis, University of Groningen, Groningen, The Netherlands, 2013.
27. Sotomayor, J.; Teixeira, M.A. Regularization of Discontinuous Vector Fields. In Proceedings of the International Conference on Differential Equations, Lisboa, Portugal, 18–23 August 1996.
28. Buzzi, C.A.; Silva, P.R.; Teixeira, M.A. A singular approach to discontinuous vector fields on the plane. *J. Differ. Equ.* **2006**, *231*, 633–655. [[CrossRef](#)]
29. Guardia, M.; Seara, T.M.; Teixeira, M.A. Generic bifurcations of low codimension of planar Filippov systems. *J. Differ. Equ.* **2011**, *250*, 1967–2023. [[CrossRef](#)]
30. Jacquemard, A.; Teixeira, M.A. On singularities of discontinuous vector fields. *Bull. Des. Sci. Math.* **2003**, *127*, 611–633. [[CrossRef](#)]
31. Llibre, J.; Silva, P.R.; Teixeira, M.A. Regularization of Discontinuous Vector Fields on R^3 via Singular Perturbation. *J. Dyn. Differ. Equ.* **2007**, *19*, 309–331. [[CrossRef](#)]
32. Llibre, J.; Silva, P.R.; Teixeira, M.A. Sliding Vector Fields via Slow-Fast Systems. *Bull. Belg. Math.-Soc.-Simon Stevin* **2008**, *15*, 851–869. [[CrossRef](#)]
33. Llibre, J.; Silva, P.R.; Teixeira, M.A. Synchronization and Non-Smooth Dynamical Systems. *J. Dyn. Differ. Equ.* **2012**, *24*, 1–12. [[CrossRef](#)]

34. Reves, C.B.; Larrosa, J.; Seara, T.M. Regularization around a generic codimension one fold-fold singularity. *J. Differ. Equ.* **2018**, *265*, 1761–1838. [[CrossRef](#)]
35. Reves, C.B.; Seara, T.M. Regularization of sliding global bifurcations derived from the local fold singularity of Filippov systems. *Discret. Contin. Dyn. Syst.* **2016**, *36*, 3545–3601. [[CrossRef](#)]
36. Tonon, D.J.; Carvalho, T. Generic Bifurcations of Planar Filippov Systems via Geometric Singular Perturbations. *Bull. Belg.-Math.-Simon Stevin* **2011**, *18*, 861–881. [[CrossRef](#)]
37. Silva, G.T.; Martins, R.M. Dynamics and stability of non-smooth dynamical systems with two switches. *Nonlinear Dyn.* **2022**, *108*, 3157–3184. [[CrossRef](#)]
38. Wang, A.L.; Xiao, Y.N. A Filippov system describing media effects on the spread of infectious diseases. *Nonlinear Anal. Hybrid Syst.* **2014**, *11*, 84–97. [[CrossRef](#)]
39. Zhang, Y.H.; Xiao, Y.N. Global dynamics for a Filippov epidemic system with imperfect vaccination. *Nonlinear Anal. Hybrid Syst.* **2020**, *38*, 100932. [[CrossRef](#)]
40. Simpson, D.J.W. *Bifurcations in Piecewise-Smooth Continuous Systems*, 1st ed.; World Scientific: Singapore, 2010.
41. Cerda, R.; Avelino, J.; Gary, C.; Tixier, P.; Lechevallier, E.; Allinne, C. Primary and secondary yield losses caused by pests and diseases: Assessment and modeling in coffee. *PLoS ONE* **2017**, *12*, e0169133. [[CrossRef](#)] [[PubMed](#)]
42. Savary, S.; Ficke, A.; Aubertot, J.; Hollier, C. Crop losses due to diseases and their implications for global food production losses and food security. *Food Secur.* **2012**, *4*, 519–537. [[CrossRef](#)]
43. Blaise, P.; Dietrich, R.; Gessler, G. Vinemild: An application-oriented model of plasmora viticola epidemics on vitis vinifera. *Acta Hort.* **1999**, *499*, 187–192. [[CrossRef](#)]
44. Thresh, J.M.; Owusu, G.K. The control of cocoa swollen shoot disease in ghana: An evaluation of eradication procedures. *Crop Prot.* **1986**, *5*, 41–52. [[CrossRef](#)]
45. Shtienberg, D.; Zilberstaine, M.; Oppenheim, D.; Levi, S.; Shwartz, H.; Kritzman, G. New Considerations for Pruning in Management of Fire Blight in Pears. *Plant Dis.* **2003**, *87*, 1083–1088. [[CrossRef](#)] [[PubMed](#)]
46. Iljon, T.; Stirling, J.; Smith, R.J. A mathematical model describing an outbreak of fire blight. In *Understanding the Dynamics of Emerging and Re-Emerging Infectious Diseases Using Mathematical Models*; Transworld Research Network: Kerala, India, 2012; Volume 2012, pp. 91–104.
47. Silva, P.R.; Llibre, J.; Teixeira, M.A. Sliding vector fields for non-smooth dynamical systems having intersecting switching manifolds. *Nonlinearity* **2015**, *28*, 493–507.
48. Jung, E.; Iwami, S.; Takeuchi, Y. Optimal control strategy for prevention of avian influenza pandemic. *J. Theor. Biol.* **2009**, *260*, 220–229. [[CrossRef](#)] [[PubMed](#)]
49. Mu, R.; Yang, Y. Global Dynamics of an Avian Influenza A(H7N9) Epidemic Model with Latent Period and Nonlinear Recovery Rate. *Comput. Math. Meth. Med.* **2018**, *2018*, 7321694. [[CrossRef](#)] [[PubMed](#)]
50. Shingo, I.; Takeuchi, Y.; Liu, X.N. Avian-human influenza epidemic model. *Math. Biosci.* **2007**, *207*, 1–25.
51. Chong, N.; Dionne, B.; Smith, R. An avian-only Filippov model incorporating culling of both susceptible and infected birds in combating avian influenza. *J. Math. Biol.* **2016**, *73*, 751–784. [[CrossRef](#)]
52. Liu, S.H.; Ruan, S.G.; Zhang, X.N. Nonlinear dynamics of avian-influenza epidemic models. *Math. Biosci.* **2017**, *283*, 118–135. [[CrossRef](#)]

Disclaimer/Publisher’s Note: The statements, opinions and data contained in all publications are solely those of the individual author(s) and contributor(s) and not of MDPI and/or the editor(s). MDPI and/or the editor(s) disclaim responsibility for any injury to people or property resulting from any ideas, methods, instructions or products referred to in the content.